Flight Dynamics Mode Identification and Model Reduction using Computational Fluid Dynamics

G. Pagliuca[*] and S. Timme[†]

University of Liverpool, Liverpool, England L69 3GH, United Kingdom

A reduced order model for free-flight test cases is presented considering the coupling of flight dynamics and aerodynamics arising from computational fluid dynamics. The formulation relies on an expansion of the full order non-linear residual function in a truncated Taylor series and subsequent projection using modes of the coupled system. Free-flight effects are included in the reduced order model by means of flight dynamics modes identified with either of two approaches. The first technique is based on the Schur decomposition of the coupled Jacobian matrix tracing the eigenvalues emerging from the rigid-body degrees-of-freedom. The second method pre-computes dynamic derivatives which are then used to identify the flight dynamics modes. The reduced order model is expanded to simulate gust encounter. All methods are applied to a two-dimensional aerofoil in transonic flow showing results for initial disturbance and gust simulations. The reduced order model is capable of reproducing full order results accurately.

I. Introduction

During aircraft design and certification, loads analyses must be performed for many flight conditions.[1] Investigating the parameter space with high-fidelity aerodynamics methods such as the Reynolds-averaged Navier-Stokes equations is prohibitive with respect to computational cost and current industrial practice relies on linear potential theory.[2] Flight dynamics is included in the loads evaluation with simple numerical methods only or neglected altogether. However, the influence of flight dynamics on the loads of a civil aircraft encountering a gust was shown recently using a linearised approach based on a modal formulation.[3] Simulations performed for transonic flow with and without flight dynamics included showed a significant impact on the loads estimation. It was also established that computational fluid dynamics (CFD) is still not ready to compete with low-fidelity aerodynamic models, such as the doublet lattice method, in terms of computing requirements.

Reduced order modelling of high-fidelity approaches is thus a good alternative to balance cost and accuracy. The research on HALE (High Altitude, Long Endurance) wings led to the development of reduced models including structural and rigid-body motions in the same modal solver.[4] System identification methods, specifically balanced realisations, were used to reduce the aerodynamic model based on the unsteady vortex lattice method. The coupled system is composed of two interacting modules reducing the structural and aerodynamic model independently. Another possible approach manipulates the full order residual with a projection on a modal basis composed of coupled structural and aerodynamic modes resulting in a monolithic reduced model.[5] The methodology was previously applied to coupled structural and aerodynamic systems using linear aerodynamics to perform gust encounter simulations and robust control.[5,6] The tools were also tested on flexible full aircraft in transonic conditions with CFD aerodynamics, using the Schur complement method to evaluate the coupled eigenmodes.[7] In particular, the Schur complement method has proven to be ready for industrial practice and it has successfully been applied to search for instabilities in the transonic regime.[8]

The model is expanded herein to account for rigid-body motions of free-flight aircraft in the transonic regime using CFD aerodynamics. This is achieved by including flight dynamics modes, also known as dynamic stability modes,[9] in the modal basis. These modes differ from the rigid-body modes since they account for

---

[*]Ph.D. Student, School of Engineering; g.pagliuca@liverpool.ac.uk.

[†]Lecturer, School of Engineering; sebastian.timme@liverpool.ac.uk.

American Institute of Aeronautics and Astronautics

the effect of aerodynamic coupling between the rigid-body degrees-of-freedom. They are similar to the modes of an aeroelastic system but based on the flight dynamics equations.[10] In a coupled structural and aerodynamic system, the calculation of aeroelastic modes can start from an in vacuum structural analysis to obtain the natural frequencies and mode shapes.[8] However, the same procedure cannot be applied for flight dynamics modes as the frequencies of the rigid-body degrees-of-freedom are all equal to zero in vacuum.[11] An additional challenge arises looking at the eigenspectrum of the Jacobian matrix of the coupled system. Eigenvalues corresponding to the flight dynamics modes depend on the flow conditions[12] and, for typical combinations of parameters, they can be found within the dense region of fluid eigenvalues. As a result, their identification among other eigenvalues is difficult.

In Section II the numerical approach for the flight dynamics modes identification is described. A Schur decomposition is applied to the coupled system and flight dynamics modes are traced starting from the rigid-body modes. An approximation of this method, based on the calculation of dynamic derivatives, is presented as well. Linear frequency-domain methods are used throughout for the CFD aerodynamics when identifying modes. Thereafter, a modal basis, built from the identified flight dynamics modes, is assembled and used to project the full order system. In Section III, results are shown for a two-dimensional test case. The reduced model is obtained for a NACA 0012 aerofoil in transonic flow solving the Euler equations while an extension to the Navier-Stokes equations is straightforward.

II. Numerical approach

A. Full order model and model reduction

Rigid-body dynamics is described by the equations of motion which are obtained directly from Newton's second law.[9] Denoting $\boldsymbol{w}_r$ the vector containing the n_r flight dynamics unknowns and $\boldsymbol{R}_r$ the corresponding non-linear residual, the flight dynamics equations are formulated as

$$\begin{aligned} \dot{\boldsymbol{w}}_r &= \boldsymbol{f}_e(\boldsymbol{w}_r) + C\boldsymbol{f}_a(\boldsymbol{w}_f, \boldsymbol{w}_r) \\ &= \boldsymbol{R}_r(\boldsymbol{w}_f, \boldsymbol{w}_r) \end{aligned} \tag{1}$$

with the vector $\boldsymbol{w}_f$ containing the n_f fluid unknowns and $\boldsymbol{f}_a$ representing aerodynamic forces. The formulation of the vector function $\boldsymbol{f}_e$ depends on the reference frame since it might include Coriolis effects[10] besides additional external forces such as gravity. The matrix C accounts for the coupling between the degrees-of-freedom and it contains information about mass and inertia properties of the system. The non-linear equations describing aerodynamics are similarly written in a semi-discrete form as

$$\dot{\boldsymbol{w}}_f = \boldsymbol{R}_f(\boldsymbol{w}_f, \boldsymbol{w}_r, \boldsymbol{u}_d) \tag{2}$$

where $\boldsymbol{u}_d$ represents a possible external disturbance such as gusts. Denoting $\boldsymbol{w} = [\boldsymbol{w}_f^T, \boldsymbol{w}_r^T]^T$ as the vector of unknowns of the coupled system, the state-space equations of dimension $n = n_f + n_r$ can be combined as

$$\dot{\boldsymbol{w}} = \boldsymbol{R}\left(\boldsymbol{w}, \boldsymbol{u}_d\right) \tag{3}$$

where $\boldsymbol{R}$ is the corresponding non-linear residual vector discretised in space.

The system in Eq. (3) is expanded in a Taylor series around an equilibrium state with $\boldsymbol{R}(\boldsymbol{w}_0) = 0$,

$$\boldsymbol{R}(\boldsymbol{w}) \approx A\,\widetilde{\boldsymbol{w}} + \frac{\partial \boldsymbol{R}}{\partial \boldsymbol{u}_d}\widetilde{\boldsymbol{u}}_d + O\left(|\widetilde{\boldsymbol{w}}|^2, |\widetilde{\boldsymbol{u}}_d|^2\right) \tag{4}$$

where $\boldsymbol{w}(t) = \boldsymbol{w}_0 + \widetilde{\boldsymbol{w}}(t)$ and accordingly $\boldsymbol{u}_d(t) = \boldsymbol{u}_{d0} + \widetilde{\boldsymbol{u}}_d(t)$. The Jacobian matrix A of dimension $n \times n$ is partitioned into blocks

$$A = \begin{pmatrix} A_{ff} & A_{fr} \\ A_{rf} & A_{rr} \end{pmatrix} \tag{5}$$

with

$$A_{ff} = \frac{\partial \boldsymbol{R}_f}{\partial \boldsymbol{w}_f} \qquad A_{fr} = \frac{\partial \boldsymbol{R}_f}{\partial \boldsymbol{w}_r} \qquad A_{rf} = C\frac{\partial \boldsymbol{f}_a}{\partial \boldsymbol{w}_f} \qquad A_{rr} = \frac{\partial \boldsymbol{f}_e}{\partial \boldsymbol{w}_r} + C\frac{\partial \boldsymbol{f}_a}{\partial \boldsymbol{w}_r} \tag{6}$$

The diagonal blocks A_{ff} and A_{rr} are fluid and flight dynamics Jacobian matrices, respectively, while the off-diagonal blocks describe the coupling terms. Specifically, the matrix A_{rf} describes the dependence of the

aerodynamic loads on the fluid unknowns, whereas A_{fr} represents fluid excitation due to the flight dynamics degrees-of-freedom. The term $\frac{\partial \boldsymbol{f}_a}{\partial \boldsymbol{w}_r}$ represents how aerodynamic forces change due to a rotation of surface normals while keeping the flow variables fixed. This term is usually small and thus neglected in the current investigation.

The system is translated into Laplace domain with complex-valued variable λ and re-arranged. The external disturbance $\boldsymbol{u}_d$ is zero for the identification of flight dynamics modes since the focus is on analysing the undisturbed system. This leads to the right and left eigenvalue problems,

$$\left(A - \lambda^{(i)}I\right)\boldsymbol{\phi}^{(i)} = 0 \qquad \text{and} \qquad \left(A^T - \lambda^{(i)}I\right)\bar{\boldsymbol{\psi}}^{(i)} = 0 \qquad \forall i,j \in [1,n] \tag{7}$$

where $(\lambda^{(i)}, \boldsymbol{\phi}^{(i)})$ and $(\lambda^{(i)}, \boldsymbol{\psi}^{(i)})$ are the corresponding eigenpairs.

The model reduction is performed by projecting the Taylor series in Eq. (4) on a smaller modal basis.[5] The bi-orthonormal bases Φ and Ψ are built by choosing m eigenvectors out of n with $m \ll n$,

$$\Phi = \left(\ \boldsymbol{\phi}^{(1)}, \quad \boldsymbol{\phi}^{(2)}, \quad \dots, \quad \boldsymbol{\phi}^{(m)} \ \right) \qquad \text{and} \qquad \Psi = \left(\ \boldsymbol{\psi}^{(1)}, \quad \boldsymbol{\psi}^{(2)}, \quad \dots, \quad \boldsymbol{\psi}^{(m)} \ \right) \tag{8}$$

The eigenvectors are normalized to satisfy the bi-orthonormality conditions resulting in

$$\langle \boldsymbol{\psi}^{(j)}, A\boldsymbol{\phi}^{(i)} \rangle = \lambda^{(i)}\delta_{ij} \qquad \text{and} \qquad \langle \boldsymbol{\psi}^{(j)}, A\bar{\boldsymbol{\phi}}^{(i)} \rangle = 0 \qquad \forall i,j \in [1,m] \tag{9}$$

where δ_{ij} is the Kronecker delta and the Hermitian inner product $\langle \boldsymbol{x}, \boldsymbol{y} \rangle$ is defined as $\bar{\boldsymbol{x}}^T \boldsymbol{y}$. The projection is performed with the transformation

$$\widetilde{\boldsymbol{w}} = \Phi \boldsymbol{z} + \bar{\Phi}\bar{\boldsymbol{z}}, \qquad \boldsymbol{z} \in \mathbb{C}^m \tag{10}$$

and pre-multiplying with the left modal basis Ψ. The reduced order model is then expressed as

$$\dot{\boldsymbol{z}} = \Lambda \, \boldsymbol{z} + \bar{\Psi}^T \frac{\partial \boldsymbol{R}}{\partial \boldsymbol{u}_d} \, \widetilde{\boldsymbol{u}}_d \tag{11}$$

where the matrix Λ is defined as a diagonal matrix containing the m eigenvalues. The modal bases in Eq. (8) must be built from flight dynamics modes and two techniques to identify these are described in the following.

B. Flight dynamics mode identification

The superscript (i) is dropped in the following discussion for clarity of notation. The right eigenvector is partitioned in aerodynamic and flight dynamics unknowns according to Eq. (5). The small eigenvalue problem of dimension n_r resulting from the flight dynamics part of the coupled equations is

$$\left[(A_{rr} - \lambda I) - \beta A_{rf} \left(A_{ff} - \lambda I\right)^{-1} A_{fr} \right]\boldsymbol{\phi}_r = S(\lambda)\boldsymbol{\phi}_r = 0 \tag{12}$$

where $S(\lambda)$ is the spectral Schur complement of A with respect to flight dynamics degrees-of-freedom. An artificial weighting factor β is introduced to gradually add the coupling effect. Newton's method solving for $(\lambda, \boldsymbol{\phi}_r)$ is used to trace the evolution of the rigid-body modes starting from zero frequency at $\beta = 0$ to the coupled eigenvalue at $\beta = 1$. The corresponding fluid part $\boldsymbol{\phi}_f$ of the eigenvector is calculated for the converged solution $(\lambda, \boldsymbol{\phi}_r)$ at $\beta = 1$ by solving

$$(A_{ff} - \lambda I)\, \boldsymbol{\phi}_f = -A_{fr}\boldsymbol{\phi}_r \tag{13}$$

The computationally expensive part of Eq. (12) is the repeated evaluation of the interaction term $A_{rf}\left(A_{ff} - \lambda I\right)^{-1} A_{fr}$ depending on the solution λ. For small-sized problems, this matrix can be computed with direct solvers whereas iterative solvers have to be applied for industrial test cases. This can lead to convergence problems if the flight dynamics eigenvalue is within the cloud of aerodynamic modes. A Taylor expansion for $\lambda = \lambda_0 + \lambda_\epsilon$ can be applied instead to improve the tracing,[8]

$$(A_{ff} - \lambda I)^{-1} = (A_{ff} - \lambda_0 I)^{-1} + \lambda_\epsilon (A_{ff} - \lambda_0 I)^{-2} + O(|\lambda_\epsilon|^2) \tag{14}$$

American Institute of Aeronautics and Astronautics

where λ_ϵ represents a small variation of λ from a reference value λ_0 given by a previously converged solution or, initially, by the rigid-body eigenvalue. The expansion can be pre-computed with matrix A_{fr} as right-hand-side using linear frequency-domain[13] (LFD) solvers and then projected with A_{rf}.

The adjoint eigenvalue problem, the solution of which is needed for the model reduction, is equivalently formulated as

$$\left[\left(A_{rr}^T - \lambda I\right) - \beta A_{fr}^T \left(A_{ff}^T - \lambda I\right)^{-1} A_{rf}^T \right] \bar{\psi}_r = 0 \tag{15}$$

Note that $\left[A_{rf}\left(A_{ff} - \lambda I\right)^{-1} A_{fr}\right]^T = A_{fr}^T(A_{ff}^T - \lambda I)^{-1}A_{rf}^T$ and thus the interaction term only needs to be pre-computed once to be applied for left and right eigenvalue problems. The fluid part of the left eigenvector is then calculated by solving the adjoint problem corresponding to Eq. (13)

$$\left(A_{ff}^T - \lambda I\right) \bar{\psi}_f = -A_{rf}^T \bar{\psi}_r \tag{16}$$

It can be shown that the interaction term corresponds to dynamic derivatives. Substituting the definition of A_{rf} into Eq. (12), the interaction term is expressed as

$$A_{rf} \left(A_{ff} - \lambda I\right)^{-1} A_{fr} = C \frac{\partial \boldsymbol{f}_a}{\partial \boldsymbol{w}_f} \left(A_{ff} - \lambda I\right)^{-1} A_{fr} \tag{17}$$

The LFD term $\left(A_{ff} - \lambda I\right)^{-1} A_{fr}$ is associated with the response of the fluid unknowns to excitations in the flight dynamics degrees-of-freedom,

$$C \frac{\partial \boldsymbol{f}_a}{\partial \boldsymbol{w}_f} \left(A_{ff} - \lambda I\right)^{-1} A_{fr} = C \frac{\partial \boldsymbol{f}_a}{\partial \boldsymbol{w}_f} \frac{\partial \boldsymbol{w}_f}{\partial \boldsymbol{w}_r} = C \frac{\partial \boldsymbol{f}_a}{\partial \boldsymbol{w}_r} = CQ \tag{18}$$

Thus, the matrix Q describes the transfer function relating flight dynamics motions (input) to the aerodynamic loads (output) by means of complex-valued dynamic derivatives of the aerodynamic system.[14, 15] The eigenvalue problem in Eq. (12) is then rewritten using dynamic derivatives as

$$\left[\left(A_{rr} - \lambda I\right) + \beta CQ \right] \boldsymbol{\phi}_r = 0 \tag{19}$$

and solved using Newton's method. The dynamic derivatives are pre-computed for non-harmonic motions corresponding to a finite number of sample points in the complex plane. Interpolation techniques are used to calculate values for points not sampled. The eigenvalue problem, Eq. (19), is theoretically identical to Eq. (12), if Q was computed for each point in the complex plane. The adjoint problem is formulated accordingly as

$$\left[\left(A_{rr}^T - \lambda I\right) + \beta Q^T C^T \right] \bar{\psi}_r = 0 \tag{20}$$

For this approach to work however, the dynamic derivatives must be computed by splitting the fluid dynamics unknowns in displacement and velocity.[7]

An approach to reduce the number of samples is obtained by neglecting the damping during the computation of the aerodynamic influence. Similarly to the P-K method,[16] which is widely used for flutter analysis, the real part of the eigenvalue is discarded when calculating the dynamic derivatives. As a consequence, the matrix Q depends on frequency only.

C. Computational fluid dynamics solver

The CFD code uses a meshless scheme to solve the Euler, laminar and Reynolds-averaged Navier-Stokes equations (with the Spalart-Allmaras turbulence model).[17, 18] The unknowns are stored at each point and the spatial discretisation is performed on a stencil of neighbouring points. Osher's approximate Riemann solver is used to evaluate the convective fluxes between each point and the points in its stencil. The gradients of the flow variables are reconstructed with the least squares method and used to provide a higher order reconstruction of the interface values for the Riemann problem. A fully implicit scheme is applied using local time stepping for convergence acceleration, while the unsteady, time-dependent equations are solved with a dual-time integration scheme. The disturbance vector $\frac{\partial \boldsymbol{R}}{\partial \boldsymbol{u}_d}$ contains the influence of the grid velocities on the residual and is calculated with central finite differences. Gusts are modelled in the flow solver with the field velocity approach.[19]

(a) Aerofoil close-up

(b) Pressure distribution
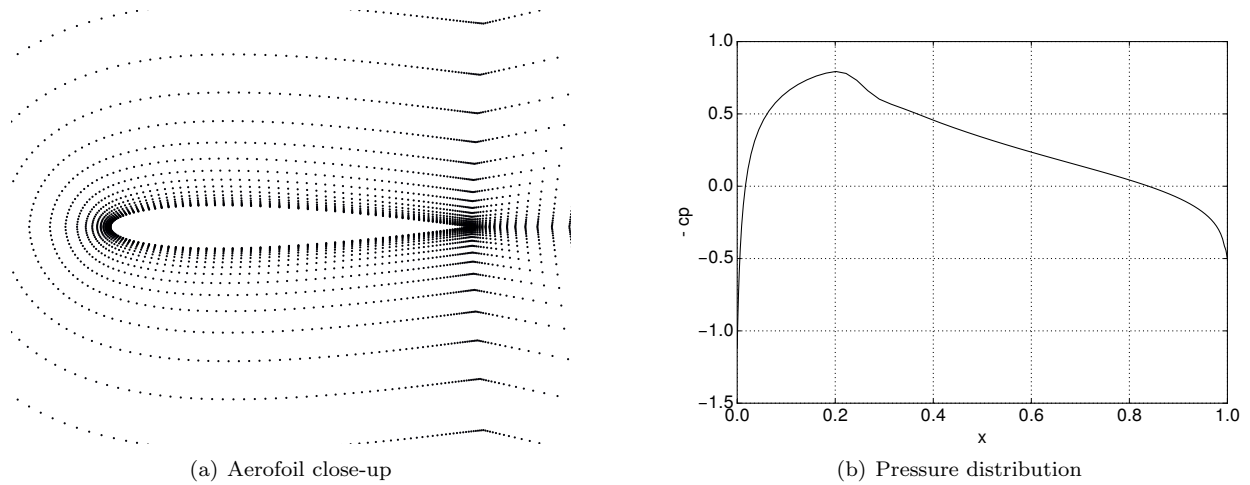
Figure 1. Point distribution for NACA 0012 aerofoil and pressure coefficient at steady state

The coupling between rigid-body dynamics and aerodynamics is performed with a modular approach at each inner iteration resulting in a strongly coupled system. At each inner iteration, the positions and velocities of grid points are modified according to the rigid motions (translation and rotation) provided by the flight dynamics module. The flight dynamics state vector is updated by integrating Newton's second law and equations for Euler angles.[3]

The linear solver used to perform LFD computations is the generalized minimal residual solver with complex arithmetic.[20] The linear solver is preconditioned using incomplete lower-upper factorization. The factorization is computed from a matrix combining Jacobian matrices arising from first and second order spacial discretizations. The blending factor is set to 0.5 which is found to be robust from numerical experiments. The preconditioner has zero fill-in to limit the memory overhead, thus retaining the same sparsity pattern as the second order Jacobian matrix.

III.   Results

Results are presented for a NACA 0012 aerofoil solving the Euler equations. The computational domain is discretized with 7860 points as shown in Fig. 1(a). The steady state is calculated at a Mach number of 0.75 and zero deg angle-of-attack. The corresponding surface pressure is given in Fig. 1(b). Assuming small variations around the initial equilibrium state, the linearised equations of motion are integrated for longitudinal dynamics.[9, 10] The flight dynamics part of the state vector contains the flight dynamics unknowns $\boldsymbol{w}_r = [u, v, q, x, z, \theta]^T$. The vertical and horizontal translations, respectively x and z, are referred to body axes[10] and the rigid rotation θ is around the centre of mass. The corresponding velocities are indicated with u, v and q. The reference length b is defined here as the semi-chord. Mass and moment of inertia of the system are denoted m and I_θ, respectively. The geometric properties of the system are expressed by means of radius of gyration $r_\theta = \sqrt{I_\theta/(mb^2)} = 0.5$ and mass ratio $\mu = \frac{m}{\pi \rho b}$. The aerodynamic drag is assumed to be constantly balanced by a thrust so that the rate of horizontal speed $\dot{u}$ is zero. Without affecting the generality of the problem, the centre of mass is located at the leading edge to have a stable system for many flow conditions.

A.   Flight dynamics mode identification

For short-term longitudinal motions, two flight dynamics modes are expected.[9] The mode corresponding to the horizontal degree-of-freedom does not contribute to the short-term response of the system and is omitted.[10] While the eigenvalue of the vertical translation mode remains close to the origin and is thus easy to calculate, the short period mode originating from the rigid rotation is more challenging to identify. The associated eigenvalue moves from the origin of the complex plane for an in vacuum mode, to a new, as yet undefined, position when aerodynamics is added. Two values of the mass ratio μ are investigated for which the system shows distinct behaviour. The results of identifying this flight dynamics mode are shown with
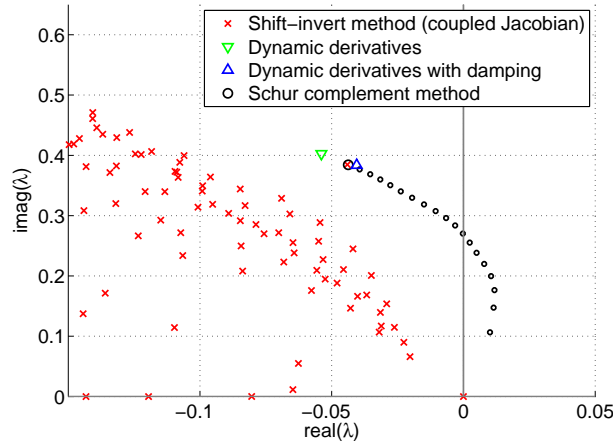
Figure 2. Eigenspectrum for identification of flight dynamics mode at $\mu = 100$.

(a) Magnitude

(b) Phase in degrees
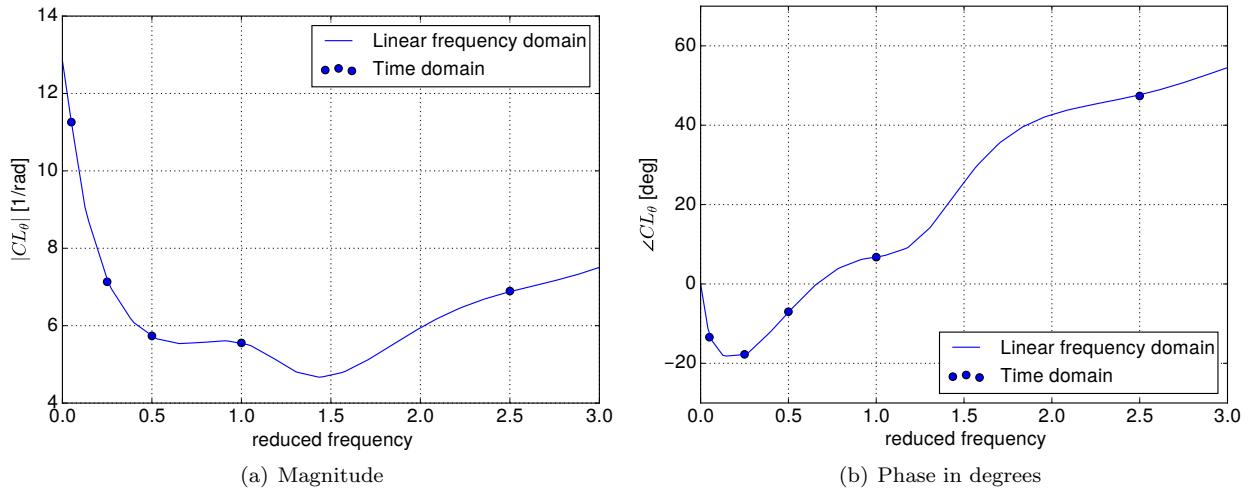
Figure 3. Magnitude and phase of lift-coefficient derivative $C_{L\theta}$ shown as representative entry of Q.

parts of the complete eigenspectrum in Figs. 2 and 4. Note that only the size of the full order problem allows a direct calculation of the eigenvalues of A and this is not the case in general. Eigenvalues close to a shift were thus extracted with the shift-invert method and included in Figs. 2 and 4 as reference.

Regarding the case with mass ratio of 100, shown in Fig. 2, the eigenvalue corresponding to the short period is outside the cloud of fluid eigenvalues. The tracing performed with the Schur complement method, described in Eq. (12), is shown with the parameter β increasing from zero to one in 20 steps. For each step Newton's method was used to calculate the eigenpair for the new value of β using the previous converged solution as initial guess. At $\beta = 0$, when all the flight dynamics eigenvalues are located in the origin of the eigenspectrum, the selection of the mode to trace is eigenvector-driven and performed by choosing a different rigid-body eigenvector of A_{rr} as initial guess. The Schur complement method provides an exact solution to the eigenvalue problem, as can be seen by comparison with the direct method. In addition, the figure includes the results from the identification method based on the approximation of the interaction matrix with dynamic derivatives. The matrix Q in Eq. (19) was pre-computed using LFD solves at 25 reduced frequencies linearly distributed in the interval 0 to 3. A linear interpolation technique is used to evaluate Q for intermediate reduced frequencies.

The dynamic derivative $C_{L\theta}$ relating the lift coefficient to the pitch angle θ is shown in Fig. 3 as a representative entry of Q. Time-domain forced motion simulations were performed as reference and good agreement was found with the LFD calculations. Solving Eq. (19), the approximation of simple harmonic motions for the dynamic derivative method (DD), i.e. by discarding the damping when calculating the

American Institute of Aeronautics and Astronautics

(a) Part of the eigenspectrum.

(b) Close-up to region of interest.
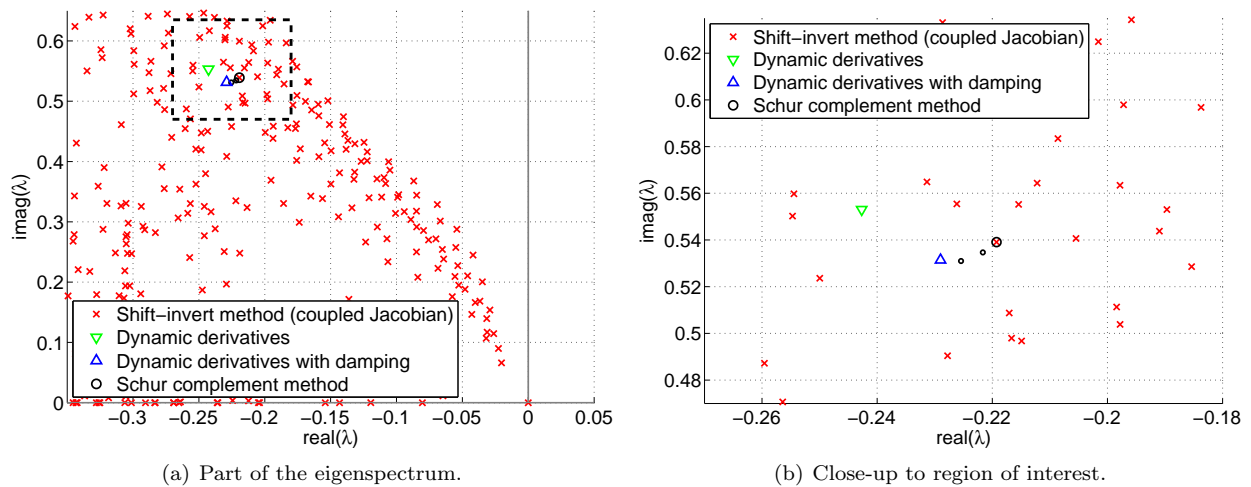
Figure 4. Eigenspectrum for identification of flight dynamics mode at $\mu = 35$.

interaction term, leads to slightly different results compared to the Schur complement method. However, this introduced error should be seen in relation to the computational cost reduced by an order of magnitude. A trade-off between the two approaches is the inclusion of damping for the calculation of the dynamic derivatives. The pre-computation of Q was extended to non-harmonic motions corresponding to a finite number of points in the complex plane. The set of 25 samples already available at zero damping was extended calculating the dynamic derivatives at the same frequencies but with a damping corresponding to the solution provided by the simple dynamic derivatives method. Linear interpolation was then used for points in the complex plane. The assumption of a linear behaviour with respect to the damping improves the final solution which is now closer to the exact result provided by the Schur complement method.

The case for the lower mass ratio of 35, when the flight dynamics eigenvalue is inside the cloud as shown in Fig. 4, is significantly more challenging. The presence of fluid eigenvalues around the target eigenvalue confuses the Schur tracer converging to fluid eigenpairs during the tracing procedure instead. This is especially true when approaching the cloud and iterative methods are used to evaluate the interaction matrix. A way to alleviate this problem, while adding to the computational cost, is to increase the number of steps for the tracing. In addition, Newton's method can be formulated to be eigenvector-driven when solving Eq. (12) by calculating the residual with the eigenvector part of the solution only by ignoring the component corresponding to the eigenvalue. In fact, distinct eigenvectors correspond to close eigenvalues. However, the number of steps cannot be increased significantly for realistic test cases and another procedure is required. The problem is overcome using the dynamic derivatives method for a first approximation of the solution. This method is not sensible to the presence of fluid eigenvalues since it uses sample points along the imaginary axis to reconstruct Q. Using the same dynamic derivatives shown in Fig. 3, the eigenvalue problem in Eq. (19) was solved for $\mu = 35$ by changing the entries in the matrix C only. The approximation of the resulting eigenvalue was further improved by adding sample points with damping value corresponding to the approximation. The resulting eigenvalue and eigenvector were used as initial solution for the Schur complement method which was capable of converging to the exact solution in few iterations.

Two modes were identified for the subsequent model reduction, specifically the short period and the mode corresponding to the vertical translation. The same techniques described in this section for the identification of the short period were applied to the translation mode. The corresponding eigenvalue stays very close to the origin of the eigenspectrum when increasing β. This means that the aerodynamic influence on this mode is weak making the identification easier.

Once the flight dynamics part of the eigenvector and the corresponding eigenvalue are available, the fluid parts are computed to assemble the modal bases. As representative entry, the pressure component of the eigenvector related to the short period at $\mu = 100$ is shown in Fig. 5. A difference of less than 0.4% was found in the pressure magnitude between eigenvectors resulting from the Schur complement method and the dynamic derivatives method.
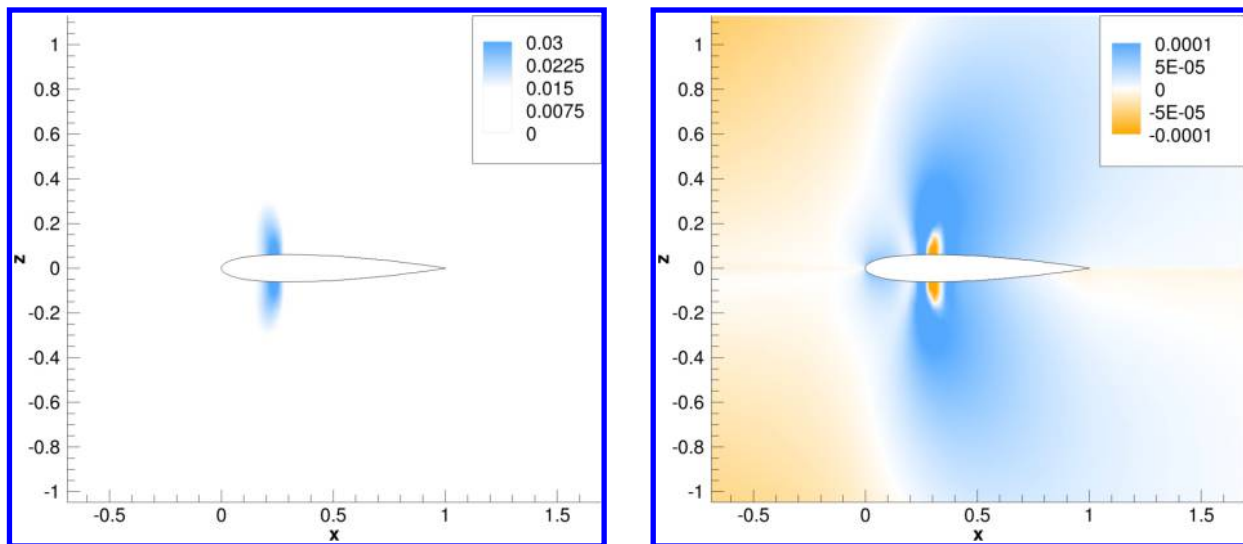
(a) Magnitude

(b) Magnitude difference due to neglecting damping

Figure 5. Difference in pressure component of right fluid eigenvector between Schur complement method and dynamic derivative method.

B. Model reduction

Subsequently, the system was projected on the modal basis to perform the model reduction. The system is investigated and results are compared to the full order model. Based on the real part of the flight dynamics eigenvalues, the system response is expected to be stable for an initial disturbance analysis. Results for an initial disturbance in the angular velocity of $q = 0.1 \deg/s$ at $\mu = 100$ are presented in Fig. 6 for the full order model (FOM) and reduced order model (ROM). Three ROMs were built using the modes provided by the Schur complement method, the dynamic derivatives approach (DD) and the dynamic derivatives method with damping (DDD). The change in the equilibrium state is reproduced by all the ROMs. Results from the reduced model based on the exact solution from the Schur complement method match the reference full order model. Small differences are visible in the first two peak values due to the broad band excitation given by the initial disturbance analysis. This can excite flight dynamics as well as the aerodynamic modes which decay leaving the system response to the dominant modes. Results from the dynamic derivatives method show an underestimation of peak values and a general frequency shift. This effect can be related to the approximations made in evaluating the real and imaginary parts of the eigenvalue. As a confirmation, the discrepancy disappears when damping is included.

The case for $\mu = 35$ presented in Fig. 7 shows a more damped response as expected from the real part of the flight dynamics eigenvalue. The new flight path is estimated by all the ROMs while some differences appear for the peak values. This results from the broadband excitation and increased aerodynamic influence. The reduced model built with the dynamic derivative method is less accurate for the transient decay even though the transition to the new equilibrium state is captured. Introducing the aerodynamic damping when estimating the dynamic derivatives improves the results, which are now closer to the full order model. However, differences still persist in the transient decay.

The reduced model was extended by introducing an external disturbance. The aim was to produce a reduced model capable of incorporating flight dynamics effects during gust encounter. Specifically, an example produced with the full order model at $\mu = 100$ is given in Fig. 8, showing loads for a gust encounter of a travelling 1–cos gust with vertical velocity $V_z = 0.1\%$ of free-stream velocity and initial starting point at the aerofoil leading edge. Two gust wavelengths with $L_g = 5$ and $L_g = 10$ chords were investigated. Including flight dynamics effects changes the peak values for lift and moment and modifies the general behaviour. Part of the energy from the disturbance goes into the system dynamics. As a results, the peak values are lowered and effects on rigid-body dynamics are significant and still visible after the disturbance had affected the system.

American Institute of Aeronautics and Astronautics

(a) Vertical displacement

(b) Angular displacement

(c) Vertical velocity
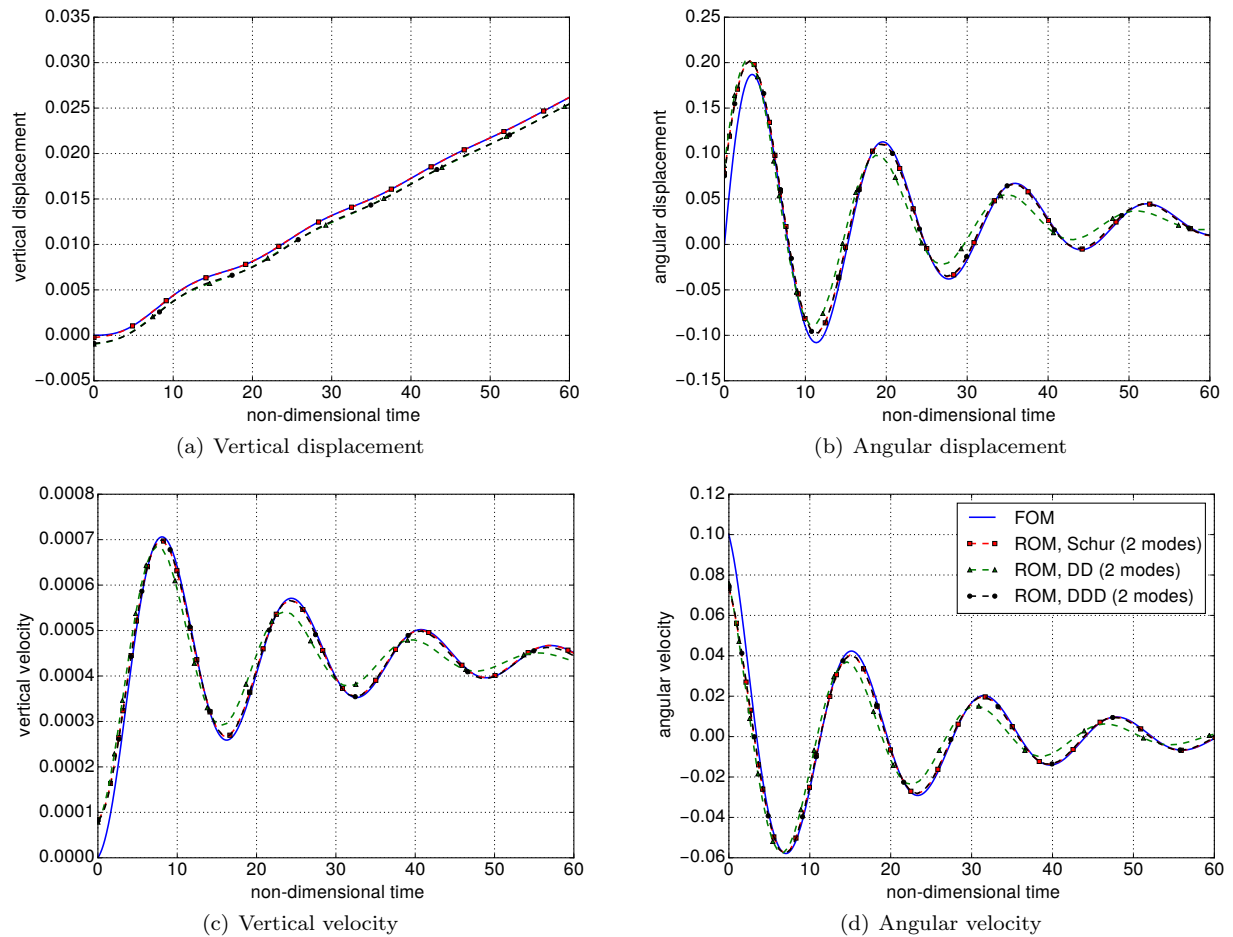
(d) Angular velocity

Figure 6. Response to initial disturbance in angular velocity of q=0.1 deg/s at $\mu = 100$.

Aerodynamic influences contained in the flight dynamics eigenpairs are able to capture the response of the system to external disturbances as depicted in Fig. 9 for the two wavelengths considered. The results from the Schur complement method are compared to the full order model showing a general agreement. Some differences arising in the peak values might depend on a non-complete description of the aerodynamic phenomena and they are more evident for angular velocity. The reduced model built with the dynamic derivatives method shows an underestimation of peak values and a shift in the frequency, when compared to the Schur complement method. The error in the identification of the flight dynamics eigenvalues, as shown in Fig. 2, affects the final results by means of Eq. (11). The decay ratio and frequency, linked to the real and imaginary parts of the eigenvalues, are therefore different from exact values given by the Schur complement method. As a confirmation, extending the calculation of dynamic derivatives to non-harmonic motions improves the final results and provides a trade-off solution between the two approaches. The trend is confirmed for a longer gust for which the differences between ROMs and FOM involve the first and second peak. Afterwards, the system dynamics is dominated by flight dynamics modes and the reduced model matches the full order model.

Regarding loads, a comparison between lift coefficients computed with reduced and full order models is presented in Fig. 10 for both initial disturbance analysis and gust encounter. The reduced model based on the Schur complement method is capable of reconstructing the aerodynamic loads due to the interaction between the system dynamics and aerodynamics. A good agreement is found for the initial disturbance analysis as shown in Fig. 10(a). Besides an underestimation of the first peak, loads are evaluated correctly in terms of both maximal values and phase. The first peak in Fig. 10(b) due to gust loads is completely ignored by the reduced model. Flight dynamics modes are insufficient to evaluate the increment in loads from pure aerodynamic disturbances like gusts. The evolution of the system is tracked when the disturbance

American Institute of Aeronautics and Astronautics

(a) Vertical displacement

(b) Angular displacement

(c) Vertical velocity
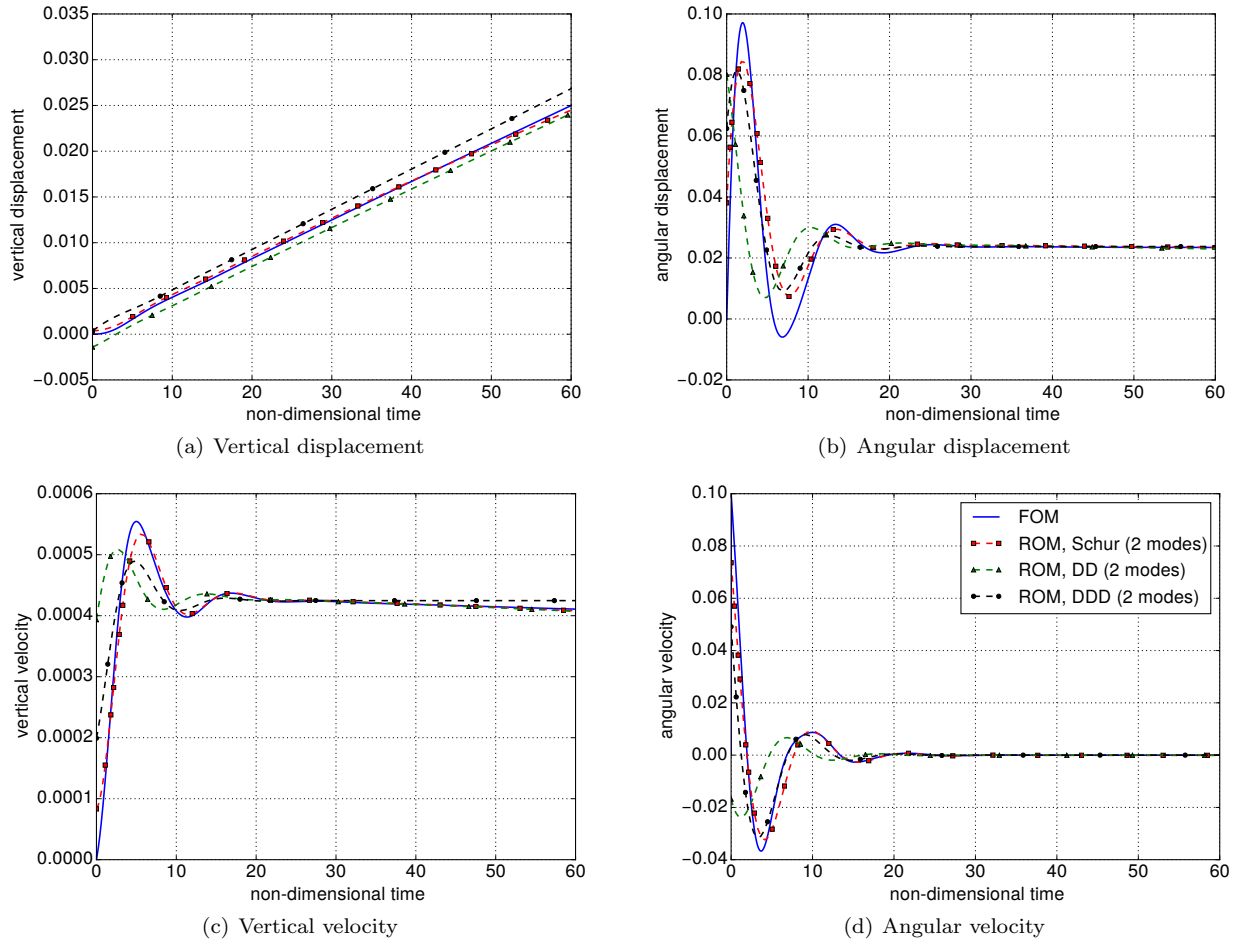
(d) Angular velocity

Figure 7. Response to initial disturbance in angular velocity of q=0.1 deg/s at $\mu = 35$.

(a) Lift coefficient

(b) Moment coefficient
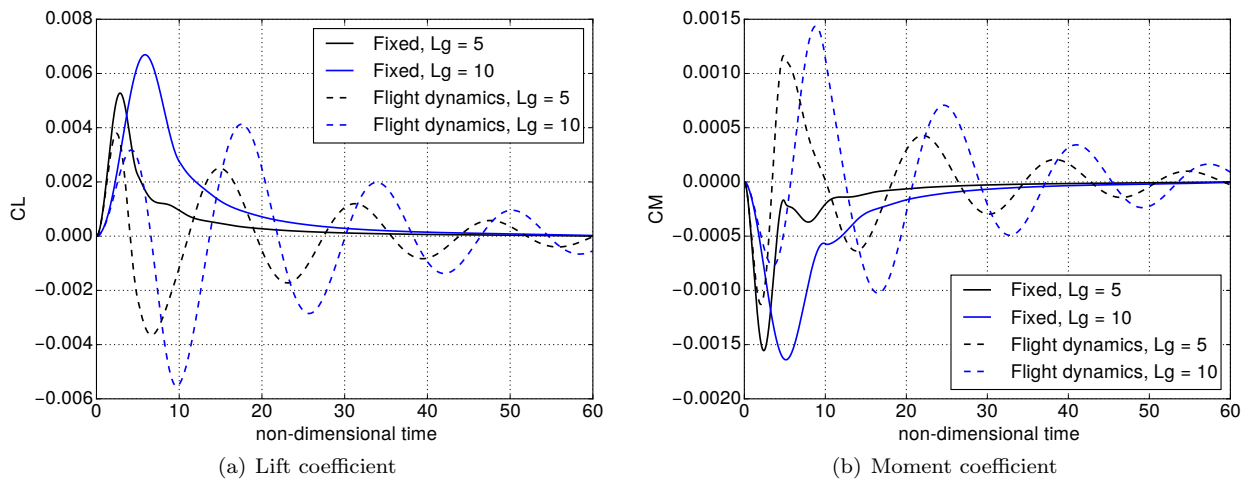
Figure 8. Effects of including flight dynamics for gust encounter.

(a) Gust wavelength $L_g = 5$
(b) Gust wavelength $L_g = 10$
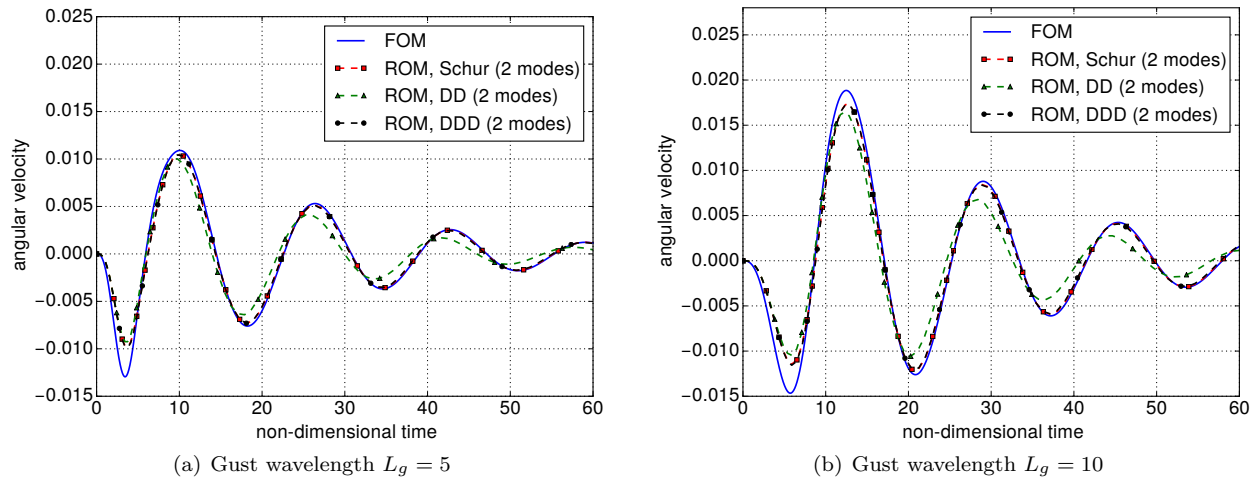
Figure 9. Gust encounter simulation for 1–cos gust with vertical velocity $V_z = 0.1\%$ of free-stream velocity and initial position at aerofoil leading edge.

(a) Initial disturbance
(b) Gust encounter with $L_g = 5$
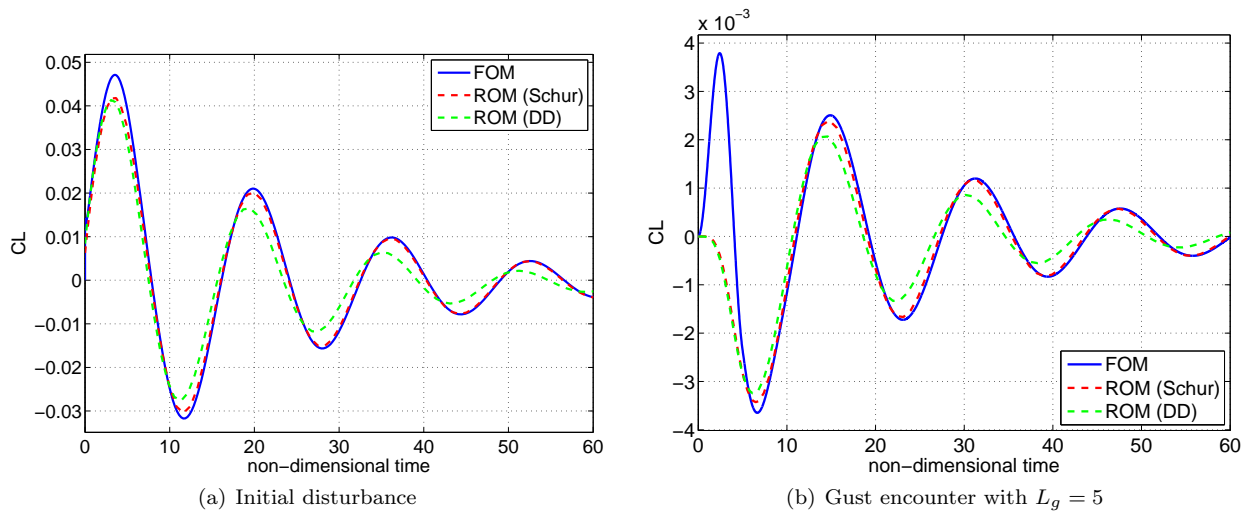
Figure 10. Loads computation performed with full and reduced order models.

is weaker and system dynamics is dominated by flight dynamics modes. The same behaviour is reported for longer gust and hence not shown. A solution to reproduce gust loads was recently offered by including gust modes in the reduced order model.[21] These modes, identified using proper orthogonal decomposition, would be in charge of retaining information for gust loads. The approximation made for the dynamic derivative method also affects loads estimation since a frequency shift and an underestimation of values is present for all the cases reported. The inclusion of the damping for the dynamic derivatives method leads to results which closely resemble the ones from the Schur complement method, thus they are not reported.

IV.   Conclusions

The paper outlines a method to include flight dynamics into a reduced order formulation and presents results for gust encounter of free-flight aircraft structures, specifically aerofoils. Computational fluid dynamics models the aerodynamics and, in particular, linear frequency-domain methods are largely used. Two solutions are proposed to identify flight dynamics modes. The first is based on the Schur complement method applied to the Jacobian matrix of the coupled aerodynamics and flight dynamics system. In terms of accuracy, results from this technique are comparable to eigenvalue extraction using direct methods. The

American Institute of Aeronautics and Astronautics

second approach is based on pre-computed dynamic derivatives for simple harmonic motions and implemented with the linear frequency-domain approach. A trade-off between these two methods is described and applied by pre-computing dynamic derivatives also for points in the complex plane. These modes identification techniques are applied to two parameter sets for which the system shows different behaviour. In particular, a strategy to cope with the identification of flight dynamics eigenvalues inside the cloud of fluid eigenvalues is presented.

The flight dynamics modes are then used to project the full order residual expanded in a Taylor series. The resulting reduced model is composed of two modes related to rigid rotation and vertical translation. The model reduction technique is capable of reproducing the effects of free flight. The reduced model is then expanded to simulate gust encounter. The effects of the aerodynamic disturbances on the system dynamics are retained even though the reduced model is not able to reconstruct gust loads, as expected, without adding additional information to model gusts. Future improvements to the modelling technique such as the inclusion of gust-related modes to fully account for gust loads and the application of these techniques to larger three-dimensional test cases, for which no comparison with direct methods is possible, are ongoing.

Acknowledgements

References

[1] EASA, "Certification specifications and acceptable means of compliance for large aeroplanes CS-25 amendment 15," 2007.

[2] Kier, T., "Comparison of unsteady aerodynamic modelling methodologies with respect to flight loads analysis," AIAA 2005-6027, 2005.

[3] Reimer, L., Ritter, M., Heinrich, R., and Kruger, W., "CFD-based gust load analysis for a free-flying flexible passenger aircraft in comparison to a DLM-based approach," AIAA 2015-2455, 2015.

[4] Hesse, H. and Palacios, R., "Model reduction in flexible-aircraft dynamics with large rigid-body motion," AIAA 2013-1895, 2013.

[5] Da Ronch, A., Badcock, K. J., Wang, Y., Wynn, A., and Palacios, R. N., "Nonlinear model reduction for flexible aircraft control design," AIAA 2012-4404, 2012.

[6] Da Ronch, A., Tantaroudas, N., Timme, S., and Badcock, K., "Model reduction for linear and nonlinear gust loads analysis," AIAA-2013-1492, 2013.

[7] Timme, S., Badcock, K. J., and Da Ronch, A., "Linear reduced order modelling for gust response analysis using the DLR-TAU code," IFASD-2013-36A, 2013.

[8] Timme, S., Marques, S., and Badcock, K. J., "Transonic aeroelastic stability analysis using a kriging-based Schur complement formulation," *AIAA Journal*, Vol. 49, No. 6, 2011, pp. 1202–1213.

[9] Wright, J. and Cooper, J., *Introduction to aircraft aeroelasticity and loads*, Wiley, 2007.

[10] Cook, M., *Flight Dynamics Principles*, Elsevier, 2007.

[11] Meirovitch, L., *Dynamics and control of structures*, Wiley, 1989.

[12] Stevens, B. and Lewis, F., *Aircraft control and simulation*, John Wiley & sons, Inc., 2003.

[13] Thormann, R. and Widhalm, M., "Linear-frequency-domain predictions of dynamic-response data for viscous transonic flows," *AIAA Journal*, Vol. 51, No. 11, 2013, pp. 2540–2557.

[14] Rodden, W. and Giesing, J. P., "Application of oscillatory aerodynamic theory to estimation of dynamic stability derivatives," *Journal of Aircraft*, Vol. 7, No. 3, 1970, pp. 272–275.

[15] Da Ronch, A., Vallespin, D., Ghoreyshi, M., and K.J., B., "Evaluation of dynamic derivatives using computational fluid dynamics," *AIAA Journal*, Vol. 50, No. 2, 2012, pp. 470–484.

[16] Hassig, H., "An approximate true damping solution of the flutter equation by determinant iteration," *Journal of Aircraft*, Vol. 8, No. 11, 1971, pp. 885–889.

[17] Kennett, D., Timme, S., Angulo, J., and Badcock, K., "Semi-meshless stencil selection for anisotropic point distributions," *International Journal of Computational Fluid Dynamics*, Vol. 26, No. 9-10, 2012, pp. 463–487.

[18] Kennett, D., Timme, S., Angulo, J., and Badcock, K., "An implicit meshless method for application in computational fluid dynamics," *International Journal for Numerical Methods in Fluids*, Vol. 71, June 2012, pp. 1007–1028.

[19] Heinrich, R. and Reimer, L., "Comparison of different approaches for gust modeling in the CFD code TAU," IFASD-2013-36B, 2013.

[20] Saad, Y. and Schultz, M. H., "GMRES: A generalized minimal residual algorithm for solving nonsymmetric linear systems," *SIAM Journal on scientific and statistical computing*, Vol. 7, No. 3, 1986, pp. 856–869.

[21] Bekemeyer, P. and Timme, S., "Reduced order gust response simulation using computational fluid dynamics," AIAA-2016-1485, 2016.